Published Ahead of Print on August 21, 2023 as 10.1212/WNL.0000000000207727

Neurology®

The most widely read and highly cited peer-reviewed neurology journal
The Official Journal of the American Academy of Neurology

AMERICAN ACADEMY OF NEUROLOGY®

Neurology Publish Ahead of Print

DOI: 10.1212/WNL.0000000000207727

Retinal Optical Coherence Tomography Features Associated With Incident and Prevalent Parkinson Disease

Author(s):

Siegfried Karl Wagner, MSc MD[1, 2]; David Romero-Bascones, BSc[2, 3]; Mario Cortina-Borja, PhD[4]; Dominic J Williamson, MSc[1, 2, 5]; Robbert R Struyven, MSc[1, 2, 5]; Yukun Zhou, MSc[1, 2, 5]; Salil Patel, MD[6]; Rimona S Weil, PhD[7]; Chrystalina A Antoniades, PhD[6]; Eric J Topol, MD[8]; Edward Korot, MD[2, 3, 9]; Paul J Foster, PhD[1, 2]; Konstantinos Balaskas, MD[1, 2]; Unai Ayala, PhD[3]; Maitane Barrenechea, PhD[3]; Iñigo Gabilondo, MD, PhD[10, 11]; Anthony HV Schapira, MD[12]; Anthony P Khawaja, PhD[1, 2]; Praveen J Patel, MD[1, 2]; Jugnoo S Rahi, PhD[1,2,4,13,14]; Alastair K Denniston, PhD[2,16,17,18]; Axel Petzold, MD, PhD[1, 2, 19]; Pearse Andrew Keane, MD[1, 2] for UK Biobank Eye & Vision Consortium

Corresponding Author:

Siegfried Karl Wagner, s.wagner@ucl.ac.uk

Affiliation Information for All Authors: 1. Institute of Ophthalmology, University College London, London, UK; 2. NIHR Biomedical Research Centre at Moorfields Eye Hospital and UCL Institute of Ophthalmology, EC1V 2PD, London, UK; 3. Biomedical Engineering Department, Faculty of Engineering (MU-ENG), Mondragon Unibertsitatea, Mondragón, Spain; 4. Great Ormond Street Institute of Child Health, University College London, London, UK; 5. Centre for Medical Image Computing, Department of Computer Science, University College London, UK; 6. NeuroMetrology Lab, Nuffield Department of Clinical Neurosciences, University of Oxford, Oxford, United Kingdom; 7. Dementia Research Centre, University College London, London, UK; 8. Department of Molecular Medicine, Scripps Research, La Jolla, CA, USA; 9. Byers Eye Institute, Stanford University, Palo Alto, CA, USA; 10. Biocruces Bizkaia Health Research Institute, Barakaldo, Spain; 11. IKERBASQUE: The Basque Foundation for Science, Bilbao, Spain; 12. Department of Clinical and Movement Neurosciences, UCL Queen Square Institute of Neurology, London, UK; 13. Great Ormond Street Hospital NHS Foundation Trust, London, UK; 14. Ulverscroft Vision Research Group, University College London, London, UK; 15. NIHR Biomedical Research Centre at UCL Great Ormond Street Institute of Child Health and Great Ormond Street Hospital, London, UK; 16. University of Birmingham, Birmingham, UK; 17. University Hospitals Birmingham NHS Foundation Trust, Birmingham, UK; 18. NIHR Birmingham Biomedical Research Centre, University of Birmingham, Birmingham, UK; 19. Queen Square Institute of Neurology, University College London, London, UK

Equal Author Contribution:

Contributions:

Siegfried Karl Wagner: Drafting/revision of the manuscript for content, including medical writing for content; Major role in the acquisition of data; Study concept or design; Analysis or interpretation of data

David Romero-Bascones: Drafting/revision of the manuscript for content, including medical writing for content; Major role in the acquisition of data; Study concept or design; Analysis or interpretation of data

Mario Cortina-Borja: Drafting/revision of the manuscript for content, including medical writing for content; Major role in the acquisition of data; Study concept or design; Analysis or interpretation of data

Dominic J Williamson: Drafting/revision of the manuscript for content, including medical writing for content; Major role in the acquisition of data; Study concept or design; Analysis or interpretation of data

Robbert R Struyven: Drafting/revision of the manuscript for content, including medical writing for content; Major role in the acquisition of data; Study concept or design; Analysis or interpretation of data

Yukun Zhou: Drafting/revision of the manuscript for content, including medical writing for content; Major role in the acquisition

of data; Study concept or design; Analysis or interpretation of data

Salil Patel: Drafting/revision of the manuscript for content, including medical writing for content; Analysis or interpretation of data

Rimona S Weil: Drafting/revision of the manuscript for content, including medical writing for content; Analysis or interpretation of data

Chrystalina A Antoniades: Drafting/revision of the manuscript for content, including medical writing for content; Analysis or interpretation of data

Eric J Topol: Drafting/revision of the manuscript for content, including medical writing for content; Analysis or interpretation of data

Edward Korot: Drafting/revision of the manuscript for content, including medical writing for content; Analysis or interpretation of data

Paul J Foster: Drafting/revision of the manuscript for content, including medical writing for content; Analysis or interpretation of data

Konstantinos Balaskas: Drafting/revision of the manuscript for content, including medical writing for content; Analysis or interpretation of data

Unai Ayala: Drafting/revision of the manuscript for content, including medical writing for content; Analysis or interpretation of data

Maitane Barrenechea: Drafting/revision of the manuscript for content, including medical writing for content; Analysis or interpretation of data

Iñigo Gabilondo: Drafting/revision of the manuscript for content, including medical writing for content; Analysis or interpretation of data

Anthony HV Schapira: Drafting/revision of the manuscript for content, including medical writing for content; Analysis or interpretation of data

Anthony P Khawaja: Drafting/revision of the manuscript for content, including medical writing for content; Analysis or interpretation of data

Praveen J Patel: Drafting/revision of the manuscript for content, including medical writing for content; Analysis or interpretation of data

Jugnoo S Rahi: Drafting/revision of the manuscript for content, including medical writing for content; Major role in the acquisition of data; Study concept or design; Analysis or interpretation of data

Alastair K Denniston: Drafting/revision of the manuscript for content, including medical writing for content; Major role in the acquisition of data; Study concept or design; Analysis or interpretation of data

Axel Petzold: Drafting/revision of the manuscript for content, including medical writing for content; Major role in the acquisition of data; Study concept or design; Analysis or interpretation of data

Pearse Andrew Keane: Drafting/revision of the manuscript for content, including medical writing for content; Major role in the acquisition of data; Study concept or design; Analysis or interpretation of data

Figure Count:

4

Table Count:

3

Search Terms:

[118] All Imaging, [161] All Movement Disorders, [165] Parkinson's disease/Parkinsonism, [188] Optic nerve, [191] Retina

Acknowledgment:

The authors thank Polly Rawlinson for project management, Curtiss Green and Louisa Wickham for information governance expertise and Tom Cusack, Simon St John-Green and Matt Barnfield for information technology support. We also acknowledge the support of Tony Ko and Reza Jafari from Topcon Healthcare for support with the use of the TABS software.

Study Funding:

Fight for Sight UK (24AZ171) Medical Research Council (MR/TR000953/1) UK Research & Innovation (MR/T040912/1, MR/T019050/1) Basque Health Department (2022333011) Wellcome Trust (205167/Z/16/Z)

Disclosure:

SK Wagner is funded by the Medical Research Council (MR/TR000953/1) and the Rank Prize. D Romero-Bascones received funding from the Basque Health Department (2022333011); M Cortina-Borja reports no disclosures; DJ Williamson reports no

disclosures; RR Struyven reports no disclosures; Y Zhou reports no disclosures; S Patel reports no disclosures; RS Weil is supported by a Wellcome Clinical Research Career Development Fellowship (205167/Z/16/Z); CA Antoniades receives funding from the NIHR, Biomedical Research Centre (BRC), UCB-OXford collaborative grant, Merck; EJ Topol reports no disclosures; E Korot reports no disclosures; PJ Foster receives salary support from NIHR through a grant to the Biomedical Research Centre at Moorfields Eye Hospital and UCL Institute of Ophthalmology; K Balaskas reports no disclosures. U Ayala receives funding from the Basque Health Department (2022333011); M Barrenechea receives funding from the Basque Health Department (2022333011); I Gabilondo receives funding from the Basque Health Department (2022333011); AHV Schapira reports no disclosures; AP Khawaja is supported by a UK Research & Innovation Future Leaders Fellowship (MR/T040912/1), an Alcon Research Institute Young Investigator Award and a Lister Institute Fellowship. AP Khawaja receives salary support from NIHR through a grant to the Biomedical Research Centre at Moorfields Eye Hospital and UCL Institute of Ophthalmology; PJ Patel reports no disclosures; JS Rahi reports no disclosures; AK Denniston reports no disclosures; A Petzold receives salary support from NIHR through a grant to the Biomedical Research Centre at Moorfields Eye Hospital and UCL Institute of Ophthalmology; PA Keane is supported by a UK Research & Innovation Future Leaders Fellowship (MR/T019050/1). PA Keane receives salary support from NIHR through a grant to the Biomedical Research Centre at Moorfields Eye Hospital and UCL Institute of Ophthalmology.

Preprint DOI:

Received Date:

2023-01-24

Accepted Date:

2023-06-14

Handling Editor Statement:

Submitted and externally peer reviewed. The handling editor was Associate Editor Peter Hedera, MD, PhD.

Abstract

Background and objectives: Cadaveric studies have shown disease-related neurodegeneration and other morphological abnormalities in the retina of individuals with Parkinson disease (PD), however it remains unclear whether this can be reliably detected with in vivo imaging. We investigated inner retinal anatomy, measured using optical coherence tomography (OCT), in prevalent PD and subsequently assessed the association of these markers with the development of PD using a prospective research cohort.

Methods: This cross-sectional analysis used data from two studies. For the detection of retinal markers in prevalent PD, we used data from AlzEye, a retrospective cohort of 154,830 patients aged 40 years and over attending secondary care ophthalmic hospitals in London, UK between 2008 and 2018. For the evaluation of retinal markers in incident PD, we used data from UK Biobank, a prospective population-based cohort where 67,311 volunteers aged 40-69 years were recruited between 2006 and 2010 and underwent retinal imaging. Macular retinal nerve fibre layer (mRNFL), ganglion cell-inner plexiform layer (GCIPL), and inner nuclear layer (INL) thicknesses were extracted from fovea--centred OCT. Linear mixed effects models were fitted to examine the association between prevalent PD and retinal thicknesses. Hazard ratios for the association between time to PD diagnosis and retinal thicknesses were estimated using frailty models.

Results: Within the AlzEye cohort, there were 700 individuals with prevalent PD and 105,770 controls (mean age 65.5 ± 13.5 years, 51.7% female). Individuals with prevalent PD had thinner

GCIPL (-2.12 μm, 95% confidence interval: -3.17, -1.07, $p = 8.2 \times 10^{-5}$) and INL (-0.99 μm, 95% confidence interval: -1.52, -0.47, $p = 2.1 \times 10^{-4}$). The UK Biobank included 50,405 participants (mean age 56.1 ± 8.2 years, 54.7% female), of whom 53 developed PD at a mean of 2653 ± 851 days. Thinner GCIPL (hazard ratio: 0.62 per standard deviation increase, 95% confidence interval: 0.46, 0.84, p=0.002) and thinner INL (hazard ratio: 0.70, 95% confidence interval: 0.51, 0.96, p=0.026) were also associated with incident PD.

Discussion: Individuals with PD have reduced thickness of the INL and GCIPL of the retina. Involvement of these layers several years before clinical presentation highlight a potential role for retinal imaging for at-risk stratification of PD.

Introduction

Parkinson disease is a heterogenous progressive movement disorder characterised by a loss of nigrostriatal dopaminergic neurons. Dopaminergic degeneration is detectable early with multimodal brain imaging, suggesting some striatal territories are affected decades before diagnosis.[1,2] Individuals with prodromal Parkinson disease have increased nigral iron deposition on susceptibility magnetic resonance imaging (MRI) and accelerated dopaminergic dysfunction on serial dopamine transport (DAT) scanning.[3,4] However, brain imaging for diagnosis and disease monitoring in Parkinson disease is limited as a scalable resource. DAT imaging is relatively costly, has modest availability, and requires intravenous contrast. MRI has shown promise for disease diagnosis and monitoring but has not yet been validated for these purposes.

Another attractive location for interrogation of dopaminergic pathology is the eye. Embryologically derived from the primitive forebrain, the retina provides a minimally invasive window into the central nervous system and can be imaged rapidly using modern high-resolution devices. The dopaminergic cells of the neurosensory retina are located in the inner plexiform (IPL) and inner nuclear layers (INL), where they mediate intercellular coupling between AII amacrine cells, horizontal cells and retinal ganglion cells.[5,6] Stimulated by the postmortem finding of reduced dopamine content in the retina of people with Parkinson disease,[7] researchers have sought evidence of retinal changes on in vivo imaging techniques, such as optical coherence tomography (OCT). OCT, an interferometry-based noncontact imaging modality (axial resolution approximately five microns) has shown diagnostic and prognostic utility in several neurological disorders[8,9] and is increasingly available in hospital and community settings[10]. Studies using OCT have revealed several potential morphological abnormalities associated with Parkinson disease but with inconsistency between studies. In a systematic review

of ten studies including a total of 690 participants, Parkinson disease was associated with reduced thickness of the macular ganglion cell-inner plexiform layer (GCIPL) and retinal nerve fibre layer (mRNFL). There was, however, a significant publication bias noted and some studies did not report key details, such as the age of controls.[11] The cell bodies of dopaminergic neurons sit at the border of INL and inner plexiform layer,[12] however the two studies reporting significant associations in a recent meta-analysis showed opposite directions of effect of Parkinson disease with the INL[11]. Most studies also exclude individuals with other medical comorbidities but the natural history of Parkinson disease may differ in individuals with other diseases, such as diabetes mellitus thus limiting the external validity of these findings to the wider patient group encountered by neurologists.[13]

In this report, we leveraged a bidirectional approach analysing retinal imaging data from individuals with Parkinson disease both prior to and post diagnosis. Our aims were firstly, to characterise inner retinal anatomy, as measured using OCT, in individuals with prevalent Parkinson disease from a large ethnically diverse real-world population study (AlzEye); and secondly to investigate the association of OCT-based measures with the development of Parkinson disease using the deeply phenotyped prospective UK Biobank (UKBB) cohort. We hypothesised that individuals with prevalent Parkinson disease would exhibit thinner GCIPL, mRNFL and INL and that this difference would be associated with incident disease.

Materials and methods

Design, participants and setting

This cross-sectional analysis used data from the AlzEye and UKBB studies to explore retinal morphology in prevalent and incident Parkinson disease respectively. AlzEye is a retrospective cohort study, where individual-level ophthalmic data has been linked with hospital admissions across England for patients, who were aged 40 years and over and had attended Moorfields Eye Hospital NHS Foundation Trust (MEH) in London, United Kingdom (UK) between January 1st 2008 and April 1st 2018. Further details about AlzEye have been published previously.[14] UKBB is a prospective population-based multicenter cohort study of approximately 500,000 participants residing in the UK and registered with the National Health Service. Participants aged 40-69 years were initially recruited between 2006 and 2010. In addition to baseline questionnaires and physical measurements, a subset of 67,311 UKBB participants additionally underwent a detailed ophthalmic assessment including retinal imaging at their initial assessment visit. Comprehensive study protocols have been published online (http://www.ukbiobank.ac.uk/resources/).

Retinal imaging

Non-mydriatic macula-centred OCT imaging was acquired by trained technicians from participants in both AlzEye and UKBB using Topcon imaging devices (Topcon Corporation, Tokyo, Japan). In AlzEye, images were acquired using four different devices (3D OCT 1000, 3D OCT 1000 Mark II, 3D OCT 2000 and Triton); for UKBB all images were acquired on the 3D OCT 1000 Mark II. All images were volume scans and covered a 6.0 mm × 6.0 mm^2 area and

had 128 horizontal B scans and 512 A scans per B scan. Images from both eyes, where available, were used. In UKBB, we only included participants who had retinal imaging acquired at the initial assessment visit (baseline instance) as this corresponded to the same time as their touchscreen questionnaire response. mRNFL, GCIPL and INL thicknesses were estimated from OCT using the Topcon Advanced Boundary Segmentation Tool (TABS) version 1.6.2.6, a software providing automated segmentation of retinal sublayers using dual-scale gradients.[15] Given previous evidence of parafoveal spatially-relevant differences in Parkinson disease and other neurodegenerative conditions, we investigated retinal sublayers for the four parafoveal subfields, as defined by the Early Treatment for Diabetic Retinopathy Study (ETDRS), as well as averages for the four inner subfields.[16] TABS provides additional metadata for each image to establish scan quality based on segmentation error, movement artefact and poor quality. For image quality control, we excluded the poorest 20% of images based on these specific image quality control metadata, applying the same method to both cohort datasets (further details in the Supplementary material).

Systemic and ocular disease variables

Parkinson disease was defined using hospital admissions data from Hospital Episode Statistics (HES), a national repository of all hospital admissions in England under the provisions of the NHS (at least 97% of hospital admissions in England[17]). HES is coded using the 10th revision of the International Classification of Diseases (ICD-10). Parkinson disease was defined as a HES episode with ICD-10 code G20. HES-based diagnostic codes for Parkinson disease have recently been validated in a subset of 20,000 participants of UKBB and had a positive predictive value of

0.84 (95% CI: 0.68, 0.94).[18] For investigating retinal markers in prevalent Parkinson disease, eligible cases were defined as images after the relevant ICD-10 code. Given previous evidence of reduced thickness of the GCIPL and mRNFL in dementia, we excluded individuals with ICD-10 codes for all-cause dementia (E512, F00, F01, F02, F03, F106, F107, G30, G310).[19] For defining incident Parkinson disease in UKBB, we excluded those who self-reported having Parkinson disease at their initial assessment visit when they had retinal imaging and then used the first hospital admission with an ICD-10 code indicating Parkinson disease as the time of disease onset. We additionally excluded those who self-reported eye disease at the initial assessment visit. Secondary exposure variables included age, sex, ethnicity, hypertension (ICD: I10, I15) and diabetes mellitus (ICD: E10, E11). Ethnicity, as self-reported by participants, was aggregated into four groups as defined by the UK Census (eTable 1). Glaucoma was defined as any patient attending the glaucoma clinic three or more times with ongoing follow-up as previously described.[14] Hypertension and diabetes mellitus were defined using HES diagnostic codes for the AlzEye analysis and through self-report at the initial assessment visit touchscreen questionnaire for UKBB. Further details regarding the Data Fields used for UKBB can be found in eTable 2.

Statistical analysis

Initial data distributions were analysed visually and statistically. Continuous variables were compared between groups using Student's *t* test and categorical variables through the *U*-Statistic permutation test of independence.[20] To examine the association between prevalent Parkinson disease and retinal morphology, we fitted linear mixed effects models with a random intercept at the individual level to account for the multilevel structure of eyes nested in participants. Models were fitted through maximum likelihood estimation and adjusted for age, sex, ethnicity group, diabetes mellitus and hypertension. To assess the risk of residual confounding (e.g. spuriously reduced retinal thickness due to individuals with Parkinson disease having more advanced diabetic eye disease), we also performed a sensitivity analysis excluding all individuals with diabetes mellitus. Degrees of freedom were estimated using Satterthwaite's approximation.[21] Data on self-reported ethnicity were missing for 19.4% subjects in the AlzEye cohort. Given previous evidence on the determinants of missingness of self-reported demographic data in healthcare, we assumed ethnicity data was missing at random[22]. We therefore performed conditional multiple imputation with chained equations ten times with five iterations using multinomial logistic regression models on all exposure and outcome variables, in their raw form, and pooled adjusted regression coefficients using Rubin's rule.[23]

To examine the association between retinal morphology and incident Parkinson disease, we estimated cause-specific adjusted hazard ratios (HR) fitting survival models including a gamma-distributed random effect on the intercept representing frailty at the individual level.[24] The at-risk period was defined from the time of retinal imaging acquisition (the UKBB initial assessment

visit data) until the earliest of death, hospital admission with a Parkinson disease diagnostic code or conclusion of the data refresh date for our UKBB application (1st December 2020). We conducted survival analysis using a complete-case approach given the small amount of missingness for ethnicity in UKBB after image quality control (<0.3% of total). Given that previous evidence has shown HES-based codes for other neurodegenerative diseases can post-date their appearance in primary care, we additionally performed a sensitivity analysis excluding all incident cases within 24 months of retinal imaging.[25] Statistical significance was set at $p<0.05$. All analyses were conducted in R version 4.1.0 (R Core Team, 2021. R Foundation for Statistical Computing, Vienna, Austria) and used the `mice`, `survival` and `lmer` packages.

Reporting is in line with the guidelines set by the Strengthening the Reporting of Observational Studies in Epidemiology (STROBE)[26] and the recommendations of the Advised Protocol for OCT Study Terminology and Elements (APOSTEL)[27,28].

Standard Protocol Approvals, Registrations, and Patient Consents

The AlzEye study has received institutional and ethical review board approval, including an exemption of participant consent (REC reference: 18/LO/1163).UKBB is conducted under the approvals of the North-West Research Ethics Committee (ref: 06/MRE08/75); specific approval was obtained for this project (application ID: 2112). All participants gave written informed consent according to the Declaration of Helsinki.

Data availability

National and international collaborations are welcomed however the data are subject to the contractual restrictions of the data sharing agreements between National Health Service Digital, Moorfields Eye Hospital and University College London and are therefore not available for access beyond the AlzEye research team. Researchers should contact the Chief Investigator at p.keane@ucl.ac.uk. Data from the United Kingdom Biobank is available to approved researchers upon application. Further information is available at https://www.ukbiobank.ac.uk/.

Results

Retinal morphology in prevalent Parkinson disease

From the AlzEye cohort of 154,830 with retinal imaging, there were 700 individuals (0.45%) who had prevalent Parkinson disease and 105,770 controls (Figure 1). Those with Parkinson disease were older, more likely to be male, hypertensive and have diabetes mellitus (Table 1, all p <0.001). In unadjusted analysis, GCIPL and INL were significantly thinner across all parafoveal locations in patients with Parkinson disease compared to controls (Figure 2, all p < 0.001). mRNFL was also thinner in individuals with Parkinson disease in all regions except the nasal subfield. Examination of those with missing ethnicity data showed that individuals, who chose not to self-report their ethnicity, were less likely to have Parkinson disease. They were also younger and less likely to have hypertension, diabetes mellitus and glaucoma. (eTable 3)

After adjustment for age, sex, ethnicity, hypertension and diabetes mellitus, individuals with prevalent Parkinson disease had significantly thinner GCIPL across all parafoveal subfields (all inner: -2.12 μm, 95% CI: -3.17, -1.07, $p = 8.2 \times 10^{-5}$). Thickness point estimates were most reduced in the inferior subfield (-2.38 μm, 95% CI: -3.54, -1.22, $p = 6.0 \times 10^{-5}$) and least reduced in the temporal subfield (-1.75 μm, 95% CI: -2.82, -0.68, $p = 0.001$). Individuals with Parkinson disease also had significantly reduced thickness of the INL across all subfields (all inner: -0.99 μm, 95% CI: -1.52, -0.47, $p = 2.1 \times 10^{-4}$), most marked at the superior subfield (-1.09 μm, 95% CI: -1.70, -0.47, $p = 5.9 \times 10^{-4}$). There was limited evidence of reduced mRNFL thickness and prevalent Parkinson disease with only a weak association seen for the inner temporal subfield (-0.69 μm, 95% CI: -1.37, -0.02, $p = 0.045$, Table 2).

Exclusion of all individuals with diabetes mellitus left a cohort of 344 individuals with Parkinson disease and 74,405 controls. Effect measures were slightly reduced but significant associations were still seen between Parkinson disease and the thickness of both the GCIPL (all inner: -1.79 μm, 95% CI: -3.30, -0.27, p = 0.020) and INL (all inner: -0.85 μm, 95% CI: -1.58, -0.13, p =0.022). There were no associations between mRNFL and prevalent Parkinson disease in this restricted group (all inner: -0.36 μm, 95% CI: -1.30, 0.57, p = 0.45).

Retinal markers and incident Parkinson disease

From 67,311 participants in UKBB who underwent extended ophthalmic assessment as part of their baseline visit, 50,405 individuals had images of sufficient quality for analysis and fit the inclusion criteria (Figure 1). The cohort had a mean age of 56.1 ± 8.2 years, 54.7% were women and people were predominantly of White self-reported ethnicity (91.4%). Fifty-three individuals developed Parkinson disease during the study period (eTable 4). Among those with incident Parkinson disease, the average time between retinal imaging and clinical presentation was 2653 ± 851 days. On adjusted survival analysis, age and male sex were significantly associated with incident Parkinson disease (Table 3). Regarding retinal markers, reduced thickness of the GCIPL was associated with incident Parkinson disease (HR = 0.62 95% CI: 0.46, 0.84 per SD increase, p = 0.002, Figure 3). There was also some evidence that thinner INL was associated with incident Parkinson disease, especially at the inferior subfield (HR = 0.66, 95% CI: 0.51, 0.86, p=0.002). The key findings of thinner GCIPL and INL being associated with greater likelihood

of developing Parkinson disease, persisted even when all those who developed Parkinson disease in the first 24 months after having had retinal imaging were excluded (Table 4).

Discussion

In this cross-sectional analysis of the AlzEye and UKBB cohorts, we first confirm earlier reports that individuals with Parkinson disease have significantly thinner GCIPL. Secondly, prevalent Parkinson disease is also associated with thinner INL, which is a novel finding. This is relevant because the INL represents the hub of dopaminergic activity in the neurosensory retina. Thirdly, we found evidence that reduced thickness of the GCIPL and, to some extent, the INL is also associated with an increased chance of developing Parkinson disease beyond that which is conferred by age, sex, ethnicity, hypertension and diabetes mellitus. Collectively, these findings strengthen the argument that neurodegenerative pathology in Parkinson disease involves the GCIPL and INL and that these retinal layers may have prognostic clinical relevance.

Prevalent Parkinson disease and INL thickness

The INL acts as a barrier to propagation of retrograde trans-synaptic axonal degeneration (RTSD) from the brain to the eye. [29] The anatomical reason for this is the network function of the INL which involves horizontal connections of bipolar cells with amacrine and horizontal cells. Data on the preservation of INL thickness have been confirmed in the second of two large meta-analyses in multiple sclerosis (MS).[8,30] In contrast to the INL, there is atrophy of the peripapillary RNFL which is robust on repeat meta-analyses over two decades and different OCT devices. Therefore, the finding of reduced INL thickness in the present cohort is not only novel, but also permits formulation of a new hypothesis of retinal neurodegeneration in Parkinson disease (Figure 4). Although the effect measure was modest (~ 1 μm), we found reduced INL thickness consistently across all parafoveal segments in prevalent Parkinson disease and in the

inferior and temporal subfields in incident Parkinson disease. Studies thus far have likely been underpowered to detect this new effect. In a 2021 meta-analysis of a total of 387 participants across four reports, only two showed significant associations between INL thickness and prevalent Parkinson disease but with opposite directions of effect.[11] While Schneider et al found a reduction in INL thickness (mean: 1.2 μm) when comparing 65 patients with Parkinson disease against age and sex-matched controls,[31] Albrecht et al noted a mean increase of 4 μm.[32] Participants in the latter work were younger on average (61.2 ± 2.0 versus 66.2 ± 12) but both had similar disease duration and severity. Dopaminergic activity in the inner retina predominantly comes from the amacrine cells,[6] which interface with retinal ganglion and AII amacrine cells. Intracellular alpha-synuclein aggregates have been found in the INL[33] and individuals with Parkinson disease have significantly reduced dopaminergic amacrine cells in the retina on immunohistochemistry.[34] Inner retinal accumulation of toxic protein aggregates provide a plausible explanation for reduced INL thickness (Figure 4). On a molecular level, toxic protein aggregates lead to increase of free radicals and oxidative stress, mitochondrial damage, and dysfunction, Ca^{2+} influx all of which lead to energy deficiency and neurodegeneration. Thus, a biologically plausible explanation for our finding could be a primary inner retinal Parkinson disease-related dopaminergic degeneration manifesting as INL thinning on OCT. This explanation reconciles our data on reduced INL thickness in Parkinson disease with the general absence of INL atrophy in non-dopaminergic neurological disorders, where inner retinal change arises from RTSD.[8]

Prevalent Parkinson disease and GCIPL thickness

We found individuals with Parkinson disease had significantly thinner GCIPL, most prominent at the superior and inferior subfields and persisting when excluding all patients with diabetes. For context, our effect estimate (-2.12 μm) equates to approximately 14 years of age in a recent UKBB cohort analysis.[35] Across 690 participants in 10 studies, Huang et al found that people with Parkinson disease had on average 3.17 μm (95% CI: -5.07, -1.26) thinner GCIPL compared to controls, with the inferior subfield exhibiting the greatest difference (-7.86 μm). GCIPL thinning has similarly been reported in Alzheimer's disease and following ischaemic stroke mediated through RTSD.[36,37] Even among neurologically healthy older individuals, a thinner GCIPL is associated with grey matter volume and brain atrophy.[38] Grey matter atrophy is found in patients with Parkinson disease, but it is heterogenous and inconsistent,[39] possibly because grey matter atrophy represents neuronal cell death[40] which is a relatively late event in Parkinson disease. Instead, animal models suggest that axonal changes are likely to be earlier events[41] and this is supported by degeneration of white matter brain connections prior to cortical atrophy in Parkinson disease.[42] In the retina, dopaminergic cell bodies are found at the border of the INL and inner plexiform layer, with axons projecting along the GCIPL. We can consider two potential mechanistic explanations for the reduced GCIPL thickness we have observed in Parkinson disease. Firstly, cerebral neurodegeneration in Parkinson disease may induce GCIPL thinning through RTSD given similar mechanisms seen in other neurodegenerative diseases. An alternative possibility is a local effect originating with dopaminergic dysfunction in the INL, or in situ axonal degeneration of the retinal ganglion cell. Although dopaminergic neurons represent <1% of all amacrine cells in the INL (density of 10-100/mm^2)[43], they reach their peak density in the parafoveal region in healthy primates (corresponding to the 1-3mm ETDRS area investigated

in this report)[34]. Moreover, retinal dopaminergic dysfunction in humans with Parkinson disease has previously been linked with death of adjacent cells, particularly ganglion cells. The dopaminergic amacrine cells couple to melanopsin-sensitive retinal ganglion cells in the GCIPL and immunohistochemistry shows that reduced dopaminergic plexi in individuals with Parkinson disease are accompanied by abnormal retinal ganglion cell morphology.[34] Immunohistochemical staining for dopamine was almost absent from the INL in Parkinson disease. Therefore, while the GCIPL and INL atrophy observed in the parafoveal region may predominantly involve other cell types, it is likely to be pathophysiologically related to dopaminergic cell death or dysfunction. Future studies are needed to determine whether progression of GCIPL atrophy in Parkinson disease is driven by retrograde mechanism from the posterior thalamus (eg lateral geniculate nucleus atrophy precedes GCIPL atrophy) or anterograde from the INL (INL thinning precedes GCIPL atrophy).

Incident Parkinson disease and inner retinal thickness

In our report, thinner INL and GCIPL were also associated with a higher risk of developing Parkinson disease. However, it should be noted that the effect sizes, especially for the INL, are small, so the practical value for an individual as a marker of early Parkinson disease is currently limited. The association between retinal layer thicknesses and incident Parkinson disease had not yet been explored; however, findings in early and prodromal Parkinson disease do corroborate our results. Reduced thickness of the GCIPL has been described in individuals with drug-naive Parkinson disease and is related to severity of disease.[44,45] Individuals with idiopathic rapid eye movement sleep behaviour disorder, a variant of prodromal Parkinson disease where >70% of

affected individuals may convert to a Lewy body disease,[46] have thinner ganglion cell complexes on OCT with the severity related to the degree of nigrostriatal dopaminergic degeneration.[47] Epidemiological patterns in other neurodegenerative diseases have also suggested inner retinal changes may occur early. In the Rotterdam Study, Mutlu et al found that individuals with thinner mRNFL on OCT had an increased risk of developing Alzheimer's dementia.[19] Another neurodegenerative explanation for the reduced inner retinal thickness observed could be glaucomatous optic neuropathy. The association between glaucoma and Parkinson disease is conflicting and a recent meta-analysis concluded that glaucoma was not associated with an increased risk of Parkinson disease [48]. In our AlzEye cohort, the prevalence of glaucoma was relatively similar in those with Parkinson disease (8.4%) and controls (7.5%) despite the group with Parkinson disease being 12 years older on average. For the UKBB analysis, we excluded all individuals with previously diagnosed glaucoma, however, it is conceivable that individuals at risk of Parkinson disease may have either undiagnosed and/or early-stage glaucoma. Ophthalmic deep phenotyping in for example, prodromal Parkinson disease would help identify the interplay between development of glaucoma and progression to a synucleinopathy.

Limitations

Firstly, for our prevalent Parkinson disease analysis, we did not have detailed clinical information about Parkinson disease status, such as diagnosis date, treatment patterns or current therapy. We were therefore not able to relate retinal morphology to disease duration or severity, although retinal thicknesses have not been shown to differ between individuals with treated and untreated Parkinson disease.[49] Secondly, our case definition of Parkinson disease was based on ICD-10 codes rather than a Parkinson disease-specific reference standard. ICD-10 codes from HES for Parkinson disease have been validated in a subset of 20,000 UKBB participants and shown to have a positive predictive value of 0.84 (0.68-0.94).[18] A separate report at a large tertiary NHS hospital showed 27% of hospital admissions of individuals with Parkinson disease did not have Parkinson disease recorded (i.e. sensitivity of 0.73).[50] Thus, our effect sizes are likely to be biased towards the null as controls may in fact have Parkinson disease. Finally, we do not have correlative OCT and retinal histology data on the proposed protein aggregation hypothesis in the INL. Such data will depend on tissue donation for research purposes by individuals with Parkinson disease who have had in-vivo OCT, such as the UK Parkinson disease Brain Bank.

In conclusion, our report demonstrates that individuals with Parkinson disease have significantly thinner GCIPL and the INL. These differences appear early, being discernible several years prior to clinical presentation. It remains unclear whether such changes relate to the increased neurodegeneration found in the brains of individuals with Parkinson disease and resulting RTSD, or could represent a primary dopaminergic degeneration focused within the inner retina with

anterior propagation of neurodegeneration. Further studies exploring the chronological sequence of retinal sublayer thickness would help elucidate the mechanism and determine whether retinal imaging could support the diagnosis, prognosis, and complex management of patients affected by Parkinson disease.

WNL-2023-000510_etab1 ---http://links.lww.com/WNL/D56

WNL-2023-000510_coinvestigator_appendix2 ---http://links.lww.com/WNL/D57

References

1. Biondetti E, Santin MD, Valabrègue R, et al. The spatiotemporal changes in dopamine, neuromelanin and iron characterizing Parkinson's disease. Brain. 2021;144:3114–3125.

2. Morrish PK, Sawle GV, Brooks DJ. An [18F]dopa–PET and clinical study of the rate of progression in Parkinson's disease. Brain. Oxford University Press (OUP); 1996;119:585–591.

3. Sun J, Lai Z, Ma J, et al. Quantitative evaluation of iron content in idiopathic rapid eye movement sleep behavior disorder. Mov Disord. 2020;35:478–485.

4. Iranzo A, Valldeoriola F, Lomeña F, et al. Serial dopamine transporter imaging of nigrostriatal function in patients with idiopathic rapid-eye-movement sleep behaviour disorder: a prospective study. Lancet Neurol. 2011;10:797–805.

5. Lee J-Y, Martin-Bastida A, Murueta-Goyena A, et al. Multimodal brain and retinal imaging of dopaminergic degeneration in Parkinson disease. Nat Rev Neurol. 2022;18:203–220.

6. Witkovsky P. Dopamine and retinal function. Doc Ophthalmol. 2004;108:17–40.

7. Harnois C, Di Paolo T. Decreased dopamine in the retinas of patients with Parkinson's disease. Invest Ophthalmol Vis Sci. 1990;31:2473–2475.

8. Petzold A, Balcer LJ, Calabresi PA, et al. Retinal layer segmentation in multiple sclerosis: a systematic review and meta-analysis. Lancet Neurol. 2017;16:797–812.

9. Vijay V, Mollan SP, Mitchell JL, et al. Using optical coherence tomography as a surrogate of measurements of intracranial pressure in idiopathic intracranial hypertension. JAMA Ophthalmol. American Medical Association (AMA); 2020;138:1264–1271.

10. Kiely PM, Cappuccio S, McIntyre E. Optometry Australia Scope of Practice Survey 2015. Clin Exp Optom. 2017;100:260–269.

11. Huang L, Zhang D, Ji J, Wang Y, Zhang R. Central retina changes in Parkinson's disease: a systematic review and meta-analysis. J Neurol. 2021;268:4646–4654.

12. Dacey DM. The dopaminergic amacrine cell. J Comp Neurol. 1990;301:461–489.

13. Komici K, Femminella GD, Bencivenga L, Rengo G, Pagano G. Diabetes Mellitus and Parkinson's Disease: A Systematic Review and Meta-Analyses. J Parkinsons Dis. 2021;11:1585–1596.

14. Wagner SK, Hughes F, Cortina-Borja M, et al. AlzEye: longitudinal record-level linkage of ophthalmic imaging and hospital admissions of 353 157 patients in London, UK. BMJ Open. BMJ; 2022;12:e058552.

15. Keane PA, Grossi CM, Foster PJ, et al. Optical Coherence Tomography in the UK Biobank Study - Rapid Automated Analysis of Retinal Thickness for Large Population-Based Studies. PLoS One. 2016;11:e0164095.

16. Early Treatment Diabetic Retinopathy Study Research Group. Photocoagulation for diabetic macular edema. Arch Ophthalmol. 1985;103:1796–1806.

17. Healthcare across the UK: A comparison of the NHS in England, Scotland, wales and northern Ireland - national audit office (NAO) report [online]. National Audit Office 2012. Accessed at: https://www.nao.org.uk/report/healthcare-across-the-uk-a-comparison-of-the-nhs-in-england-scotland-wales-and-northern-ireland/. Accessed August 2, 2022.

18. Website [online]. Accessed at: (https://biobank.ctsu.ox.ac.uk/crystal/ukb/docs/alg_outcome_pdp.

19. Mutlu U, Colijn JM, Ikram MA, et al. Association of retinal neurodegeneration on optical coherence tomography with dementia: A population-based study. JAMA Neurol. American Medical Association (AMA); 2018;75:1256–1263.

20. Berrett TB, Samworth R. USP: an independence test that improves on Pearson's chi-squared and the G-test. Apollo - University of Cambridge Repository; Epub 2021. Accessed at: https://www.repository.cam.ac.uk/handle/1810/330630.

21. Satterthwaite FE. An approximate distribution of estimates of variance components. Biometrics. 1946;2:110–114.

22. Tsiampalis T, Panagiotakos DB. Missing-data analysis: socio- demographic, clinical and lifestyle determinants of low response rate on self- reported psychological and nutrition related multi- item instruments in the context of the ATTICA epidemiological study. BMC Med Res Methodol. Springer Science and Business Media LLC; 2020;20:148.

23. van Buuren S. Multiple imputation of discrete and continuous data by fully conditional specification. Stat Methods Med Res. 2007;16:219–242.

24. Hens N, Wienke A, Aerts M, Molenberghs G. The correlated and shared gamma frailty model for bivariate current status data: an illustration for cross-sectional serological data. Stat Med. Wiley; 2009;28:2785–2800.

25. Brown A, Kirichek O, Balkwill A, et al. Comparison of dementia recorded in routinely collected hospital admission data in England with dementia recorded in primary care. Emerg Themes Epidemiol. 2016;13:11.

26. von Elm E, Altman DG, Egger M, et al. The Strengthening the Reporting of Observational Studies in Epidemiology (STROBE) Statement: guidelines for reporting observational studies. Int J Surg. Elsevier BV; 2014;12:1495–1499.

27. Aytulun A, Cruz-Herranz A, Aktas O, et al. APOSTEL 2.0 recommendations for reporting quantitative optical coherence tomography studies. Neurology. Ovid Technologies (Wolters Kluwer Health); 2021;97:68–79.

28. Cruz-Herranz A, Balk LJ, Oberwahrenbrock T, et al. The APOSTEL recommendations for reporting quantitative optical coherence tomography studies. Neurology. 2016;86:2303–2309.

29. Balk LJ, Steenwijk MD, Tewarie P, et al. Bidirectional trans-synaptic axonal degeneration in the visual pathway in multiple sclerosis. J Neurol Neurosurg Psychiatry. 2015;86:419–424.

30. Petzold A, de Boer JF, Schippling S, et al. Optical coherence tomography in multiple sclerosis: a systematic review and meta-analysis. Lancet Neurol. 2010;9:921–932.

31. Schneider M, Müller H-P, Lauda F, et al. Retinal single-layer analysis in Parkinsonian syndromes: an optical coherence tomography study. J Neural Transm. 2014;121:41–47.

32. Albrecht P, Müller A-K, Südmeyer M, et al. Optical coherence tomography in parkinsonian syndromes. PLoS One. 2012;7:e34891.

33. Bodis-Wollner I, Kozlowski PB, Glazman S, Miri S. A-synuclein in the inner retina in parkinson disease. Ann Neurol. Wiley; 2014;75:964–966.

34. Ortuño-Lizarán I, Sánchez-Sáez X, Lax P, et al. Dopaminergic Retinal Cell Loss and Visual Dysfunction in Parkinson Disease. Ann Neurol. 2020;88:893–906.

35. Khawaja AP, Chua S, Hysi PG, et al. Comparison of Associations with Different Macular Inner Retinal Thickness Parameters in a Large Cohort: The UK Biobank. Ophthalmology. 2020;127:62–71.

36. Jindahra P, Petrie A, Plant GT. The time course of retrograde trans-synaptic degeneration following occipital lobe damage in humans. Brain. 2012;135:534–541.

37. Chan VTT, Sun Z, Tang S, et al. Spectral-domain OCT measurements in Alzheimer's disease: A systematic review and meta-analysis. Ophthalmology. Elsevier BV; 2019;126:497–510.

38. Mejia-Vergara AJ, Karanjia R, Sadun AA. OCT parameters of the optic nerve head and the retina as surrogate markers of brain volume in a normal population, a pilot study. J Neurol Sci. 2021;420:117213.

39. Weil RS, Hsu JK, Darby RR, Soussand L, Fox MD. Neuroimaging in Parkinson's disease dementia: connecting the dots. Brain Commun. 2019;1:fcz006.

40. Rossor MN, Fox NC, Freeborough PA, Roques PK. Slowing the progression of Alzheimer disease: monitoring progression. Alzheimer Dis Assoc Disord. 1997;11 Suppl 5:S6-9.

41. Chung CY, Koprich JB, Siddiqi H, Isacson O. Dynamic changes in presynaptic and axonal transport proteins combined with striatal neuroinflammation precede dopaminergic neuronal loss in a rat model of AAV alpha-synucleinopathy. J Neurosci. 2009;29:3365–3373.

42. Zarkali A, McColgan P, Leyland L-A, Lees AJ, Weil RS. Visual Dysfunction Predicts Cognitive Impairment and White Matter Degeneration in Parkinson's Disease. Mov Disord. 2021;36:1191–1202.

43. Popova E. Role of dopamine in retinal function. University of Utah Health Sciences Center; 2020.

44. Lee J-Y, Ahn J, Yoon EJ, Oh S, Kim YK, Jeon B. Macular ganglion-cell-complex layer thinning and optic nerve integrity in drug-naïve Parkinson's disease. J Neural Transm. 2019;126:1695–1699.

45. Ahn J, Lee J-Y, Kim TW, et al. Retinal thinning associates with nigral dopaminergic loss in de novo Parkinson disease. Neurology. 2018;91:e1003–e1012.

46. Postuma RB, Gagnon J-F, Bertrand J-A, Génier Marchand D, Montplaisir JY. Parkinson risk in idiopathic REM sleep behavior disorder: preparing for neuroprotective trials. Neurology. 2015;84:1104–1113.

47. Lee J-Y, Ahn J, Oh S, et al. Retina thickness as a marker of neurodegeneration in prodromal lewy body disease. Mov Disord. 2020;35:349–354.

48. Zhao B, Cheung R, Malvankar-Mehta MS. Risk of Parkinson's disease in glaucoma patients: a systematic review and meta-analysis. Curr Med Res Opin. Informa UK Limited; 2022;38:955–962.

49. Sen A, Tugcu B, Coskun C, Ekinci C, Nacaroglu SA. Effects of levodopa on retina in Parkinson disease. Eur J Ophthalmol. 2014;24:114–119.

50. Muzerengi S, Rick C, Begaj I, et al. Coding accuracy for Parkinson's disease hospital admissions: implications for healthcare planning in the UK. Public Health. 2017;146:4–9.

Characteristic		Parkinson disease (*n*=700)	Controls (*n*=105,770)	*p*-value
Age (years)		77.5 +/- 8.0	65.4 +/- 13.5	**<0.001**
Women (*n* (%))		292 (41.7)	54,717 (51.7)	**<0.001**
Ethnicity (*n* (%))	**South Asian**	154 (22.0)	18,188 (17.2)	**0.026**
	Black	55 (7.9)	9,249 (8.7)	
	Other/Mixed	99 (14.1)	17,510 (16.6)	
	White	292 (41.7)	40,316 (38.1)	
	Unknown	100 (14.3)	20,507 (19.4)	
Hypertension (*n* (%))		558 (79.7)	53,010 (50.1)	**<0.001**
Diabetes mellitus (*n* (%))		356 (50.9)	31,365 (29.7)	**<0.001**
Glaucoma (n (%))		59 (8.4)	7,964 (7.5)	0.39
mRNFL (μm)	**All inner subfields**	24.7 +/- 8.0	25.4 +/- 8.4	**<0.001**
	Inner superior	26.6 +/- 9.8	27.0 +/- 9.5	**0.017**
	Inner nasal	25.0 +/- 9.3	25.2 +/- 10.0	0.21
	Inner temporal	19.9 +/- 8.0	21.0 +/- 8.7	**<0.001**
	Inner inferior	27.4 +/- 9.6	28.5 +/- 9.6	**<0.001**
GCIPL (μm)	**All inner subfields**	77.1 +/- 15.0	82.9 +/- 13.9	**<0.001**
	Inner superior	76.9 +/- 17.0	83.0 +/- 15.4	**<0.001**
	Inner nasal	78.0 +/- 16.0	84.0 +/- 15.1	**<0.001**
	Inner temporal	76.6 +/- 15.5	81.4 +/- 14.0	**<0.001**
	Inner inferior	76.9 +/- 16.9	83.3 +/- 15.3	**<0.001**
INL (μm)	**All inner subfields**	39.9 +/- 6.3	41.1 +/- 6.8	**<0.001**
	Inner superior	40.0 +/- 7.7	41.5 +/- 8.0	**<0.001**
	Inner nasal	41.0 +/- 7.0	42.1 +/- 7.8	**<0.001**
	Inner temporal	37.9 +/- 8.0	39.2 +/- 7.9	**<0.001**
	Inner inferior	40.5 +/- 7.7	41.8 +/- 7.9	**<0.001**

Table 1: Baseline characteristics of the AlzEye cohort by Parkinson disease status. Note that all results are at the level of the individual with the summary values for retinal imaging representing the means of the two eyes. Except where indicated, all characteristic results are shown as mean +/- standard deviation.

INL: inner nuclear layer, GCIPL: macular ganglion cell-inner plexiform layer, mRNFL: macular retinal nerve fibre layer, SD: standard deviation.

Prevalent Parkinson disease		AlzEye – all (*n* cases = 700)		AlzEye – no diabetes mellitus (*n* cases = 344)	
Characteristic		**Layer thickness difference (95% CI)**	***p*-value**	**Layer thickness difference (95% CI)**	***p*-value**
mRNFL (µm)	**All subfields**	-0.39 (-1.04, 0.26)	0.24	-0.36 (-1.30, 0.57)	0.45
	Inner superior	-0.26 (-1.00, 0.47)	0.48	-0.36 (-1.41, 0.69)	0.50
	Inner nasal	-0.19 (-0.97, 0.59)	0.63	-0.02 (-1.16, 1.12)	0.97
	Inner temporal	-0.69 (-1.37, -0.02)	**0.045**	-0.78 (-1.73, 0.17)	0.11
	Inner inferior	-0.41 (-1.16, 0.34)	0.28	-0.26 (-1.33, 0.82)	0.64
GCIPL (µm)	**All subfields**	-2.12 (-3.17, -1.07)	**8.2×10^{-5}**	-1.79 (-3.30, -0.27)	**0.020**
	Inner superior	-2.36 (-3.52, -1.19)	**7.2×10^{-5}**	-2.07 (-3.73, -0.41)	**0.015**
	Inner nasal	-2.01 (-3.15, -0.87)	**5.6×10^{-4}**	-1.54 (-3.18, 0.09)	0.06
	Inner temporal	-1.75 (-2.82, -0.68)	**0.001**	-1.49 (-3.03, 0.04)	0.06
	Inner inferior	–2.38 (-3.54, -1.22)	**6.0×10^{-5}**	-1.90 (-3.56, -0.24)	**0.025**
INL (µm)	**All subfields**	-0.99 (-1.52, -0.47)	**2.1×10^{-4}**	-0.85 (-1.58, -0.13)	**0.022**
	Inner superior	-1.09 (-1.70, -0.47)	**5.9×10^{-4}**	-1.06 (-1.92, -0.21)	**0.015**
	Inner nasal	-1.00 (-1.61, -0.39)	**0.001**	-0.79 (-1.63, 0.05)	0.07
	Inner temporal	-0.99 (-1.60, -0.38)	**0.001**	-1.00 (-1.83, -0.16)	**0.019**
	Inner inferior	-0.89 (-1.51, -0.28)	**0.004**	-0.59 (-1.44, 0.26)	0.18

Table 2: Association between retinal layer thickness and prevalent Parkinson disease. Pooled adjusted regression coefficients estimated using linear mixed effects modelling retinal layer thickness against Parkinson disease. All models are adjusted for age, sex, ethnicity, diabetes mellitus and hypertension. CI: confidence interval, INL: inner nuclear layer, GCIPL: macular ganglion cell-inner plexiform layer, mRNFL: macular retinal nerve fibre layer

Variable		Incident Parkinson disease					
		mRNFL (all inner subfields)		GCIPL (all inner subfields)		INL (all inner subfields)	
		HR (95% CI)	*p*-value	HR (95% CI)	*p*-value	HR (95% CI)	*p*-value
Retinal sublayer	Per SD increase	0.81 (0.60, 1.11)	0.19	0.62 (0.46, 0.84)	0.002	0.70 (0.51, 0.96)	0.026
Age	Per decile	1.21 (1.15, 1.28)	4.6×10^{-13}	6.10 (3.62, 10.28)	1.2×10^{-11}	1.22 (1.15, 1.28)	1.7×10^{-13}
Sex	Female	Reference		Reference		Reference	
	Male	3.91 (2.11, 7.24)	1.5×10^{-5}	4.11 (2.21, 7.66)	8.4×10^{-6}	4.54 (2.39, 8.60)	3.5×10^{-6}
Ethnicity	Asian (South)	Reference		Reference		Reference	
	Black	2.74 (0.12, 62.90)	0.53	2.12 (0.09, 52.5)	0.65	3.26 (0.14, 76.77)	0.46
	White	1.45 (0.12, 18.15)	0.77	1.52 (0.11, 20.2)	0.75	1.48 (0.11, 19.28)	0.77
	Other/Mixed	0.98 (0.03, 32.57)	0.99	1.03 (0.11, 20.24)	0.99	1.01 (0.03, 35.25)	1.0
Diabetes mellitus	Absent	Reference		Reference		Reference	
	Present	1.15 (0.25, 5.28)	0.86	1.04 (0.22, 4.80)	0.96	1.08 (0.23, 4.99)	0.92
Hypertension	Absent	Reference		Reference		Reference	
	Present	0.77 (0.39, 1.54)	0.46	0.77 (0.38, 1.55)	0.46	0.76 (0.38, 1.52)	0.43

Table 3: Association between retinal layer thickness and exposure variables with incident Parkinson disease. Hazard ratios for all exposures variables derived from multivariable frailty models. Models for average inner subfield thickness for the macular retinal nerve fiber, ganglion cell-inner plexiform and inner nuclear layers are shown. GCIPL: ganglion cell-inner plexiform layer, HR: hazard ratio, INL: inner nuclear layer, mRNFL: macular retinal nerve fiber layer, SD: standard deviation.

Incident Parkinson disease		Unadjusted		Adjusted		Adjusted - late diagnosis	
		HR (95% CI)	*p* value	HR (95% CI)	*p*-value	HR (95% CI)	*p*-value
mRNFL (μm) (per SD increase)	**All subfields**	0.81 (0.62, 1.06)	0.13	0.81 (0.60, 1.11)	0.19	0.83 (0.61, 1.12)	0.23
	Inner superior	0.85 (0.65, 1.10)	0.21	0.85 (0.62, 1.15)	0.29	0.86 (0.63, 1.16)	0.32
	Inner nasal	0.87 (0.64, 1.18)	0.37	0.83 (0.58, 1.19)	0.31	0.85 (0.60, 1.20)	0.36
	Inner temporal	0.96 (0.74, 1.23)	0.73	1.04 (0.79, 1.35)	0.80	1.05 (0.80, 1.37)	0.73
	Inner inferior	0.79 (0.63, 1.00)	**0.047**	0.77 (0.60, 1.00)	0.05	0.78 (0.60, 1.01)	0.06
GCIPL (μm) (per SD increase)	**All inner subfields**	0.54 (0.42, 0.71)	**8.0×10^{-6}**	0.62 (0.46, 0.84)	**0.002**	0.64 (0.48, 0.87)	**0.004**
	Inner superior	0.57 (0.45, 0.74)	**1.5×10^{-5}**	0.64 (0.48, 0.85)	**0.002**	0.65 (0.49, 0.87)	**0.004**
	Inner nasal	0.54 (0.42, 0.71)	**5.5×10^{-6}**	0.67 (0.50, 0.90)	**0.008**	0.69 (0.52, 0.93)	**0.014**
	Inner temporal	0.66 (0.51, 0.87)	**0.003**	0.70 (0.51, 0.94)	**0.019**	0.73 (0.54, 0.98)	**0.038**
	Inner inferior	0.57 (0.45, 0.72)	**2.7×10^{-6}**	0.61 (0.47, 0.81)	**4.9×10^{-4}**	0.62 (0.47, 0.82)	**7.6×10^{-4}**
INL (μm) (per SD increase)	**All subfields**	0.85 (0.66, 1.11)	0.24	0.70 (0.51, 0.96)	**0.026**	0.70 (0.51, 0.97)	**0.032**
	Inner superior	0.88 (0.68, 1.14)	0.32	0.76 (0.56, 1.04)	0.08	0.76 (0.56, 1.04)	0.09
	Inner nasal	1.07 (0.82, 1.39)	0.62	0.92 (0.67, 1.26)	0.61	0.94 (0.67, 1.29)	0.70
	Inner temporal	0.80 (0.62, 1.05)	0.11	0.67 (0.49, 0.92)	**0.013**	0.67 (0.48, 0.92)	**0.013**
	Inner inferior	0.79 (0.63, 0.99)	**0.037**	0.66 (0.51, 0.86)	**0.002**	0.66 (0.50, 0.86)	**0.002**

Table 4: Association between retinal layer thickness and incident Parkinson disease. Hazard ratios derived from mixed effects Cox proportional hazards modelling time to diagnosis of Parkinson disease against retinal layer thicknesses. Adjusted models control for age, sex, ethnicity, diabetes mellitus and hypertension. Late diagnosis model excludes all individuals developing Parkinson disease within 2 years of retinal imaging. CI: confidence interval, HR: hazard ratio, INL: inner nuclear layer, GCIPL: macular ganglion cell-inner plexiform layer, mRNFL: macular retinal nerve fibre layer

Figure legends

Figure 1: Flow chart detailing inclusion and exclusion of participants in both AlzEye and UK Biobank. PD: Parkinson disease.

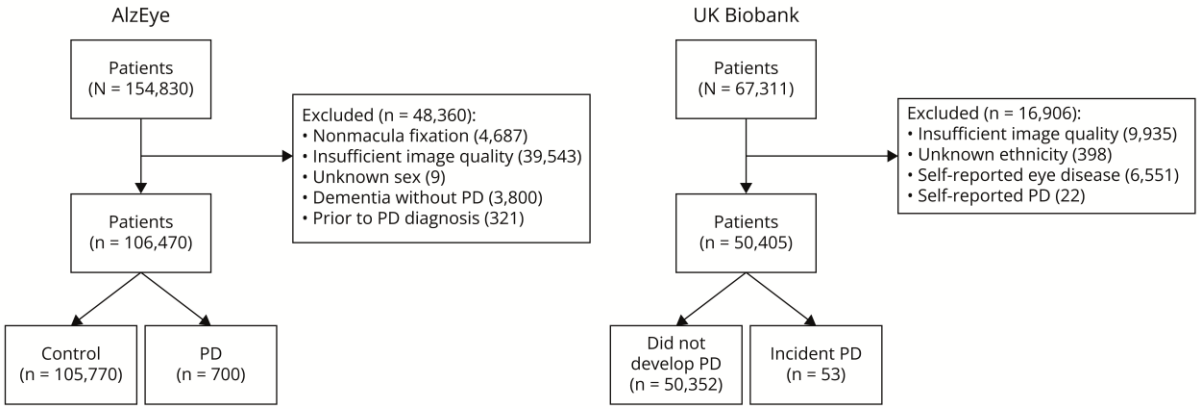

Figure 2: Distribution of retinal sublayer thicknesses in AlzEye and UK Biobank. Raincloud plots consisting of a density, box-whisker, and scatter plots for AlzEye (A-C) and UK Biobank (D-F) for individual retinal sublayers. Scatter points represent the mean of both eyes (where available) per participant. To improve visibility, a random 2% of control participants are illustrated.

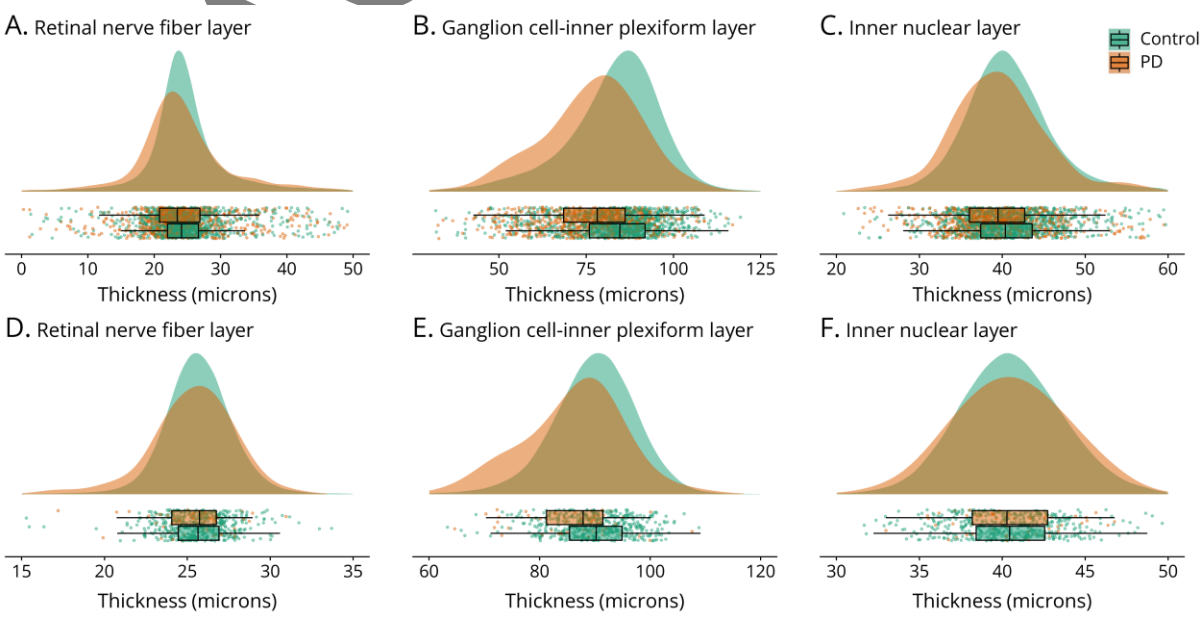

Figure 3: Summary of findings for prevalent and incident Parkinson disease. Values are shown per parafoveal region and for the average of all inner segments (small donut). The effect measure corresponds to a color scale with warm colors indicating lower numbers.

II: inner inferior, IN: inner nasal, IS: inner superior, IT: inner temporal INL: inner nuclear layer, GCIPL: macular ganglion cell-inner plexiform layer, mRNFL: macular retinal nerve fiber layer

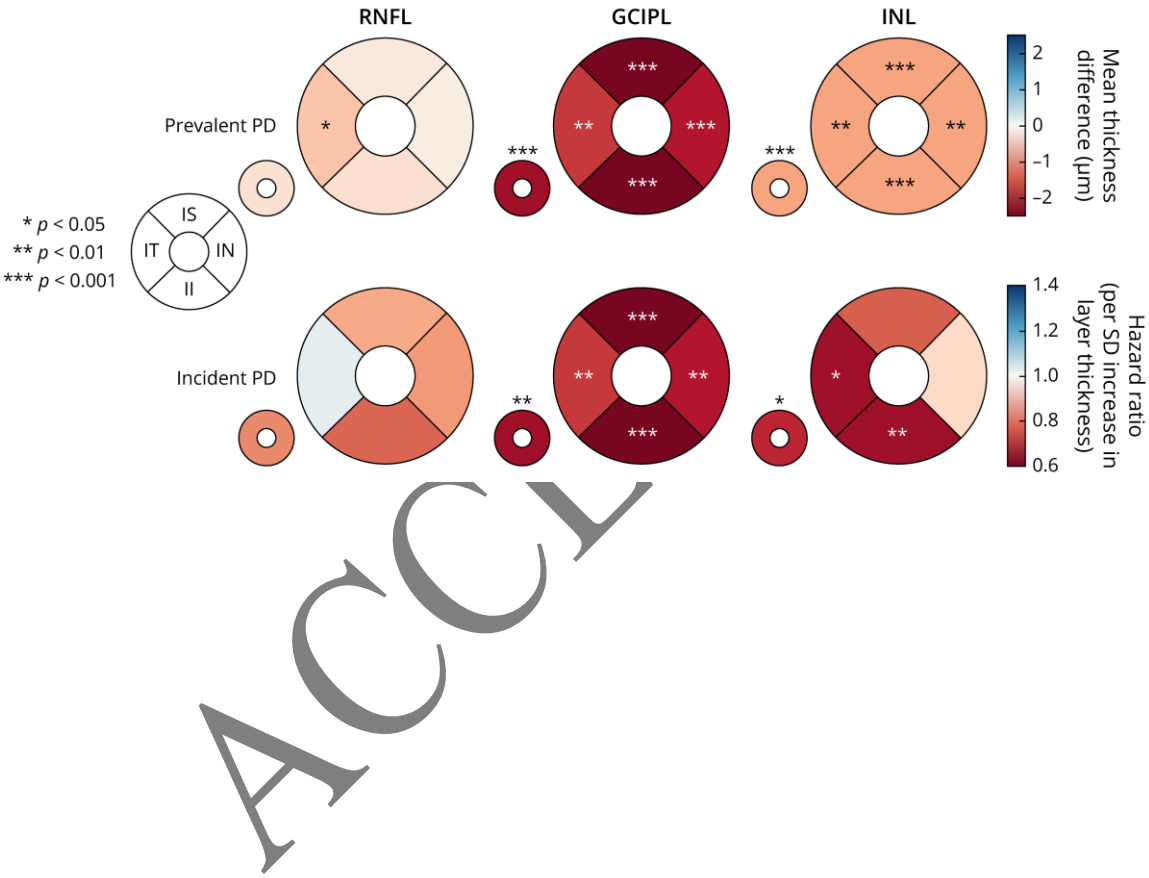

Figure 4: Illustration of cell type distribution in the retina. An example optical coherence tomography scan of the nasal macula adjacent to a schematic detailing interactions with dopaminergic amacrine cells. Dopaminergic cells (1) have dense plexi positioned throughout the inner plexiform and inner nuclear layers. They are pre-synaptic to amacrine AII cells (2) and some dopaminergic processes project towards the photoreceptor layer where they interact with horizontal cells (3). They are postsynaptic to bipolar cells (4). Previous work has demonstrated aggregation of proteins, including α synuclein, within the inner nuclear layer (5), which could result in impairment of nearby ganglion cells.

INL: inner nuclear layer, GCIPL: macular ganglion cell-inner plexiform layer, PRL: photoreceptor layer, RPE: retinal pigment epithelium, RNFL: retinal nerve fiber layer

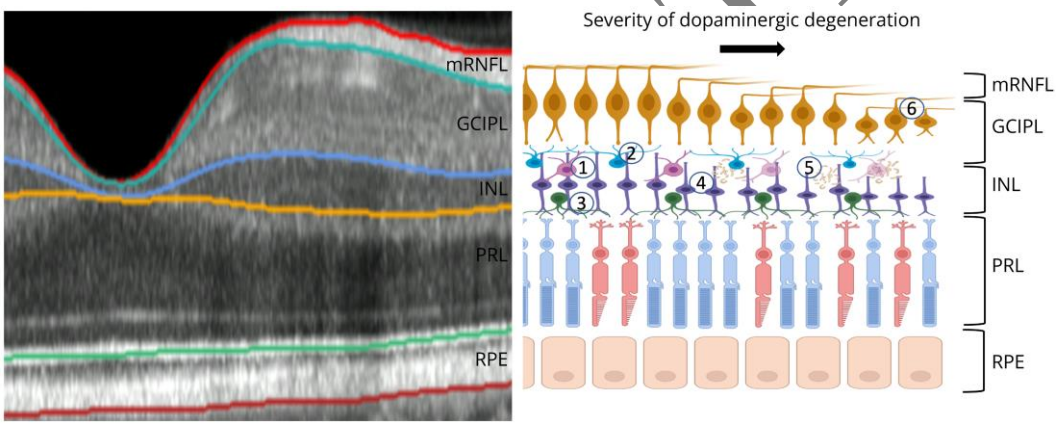

Retinal Optical Coherence Tomography Features Associated With Incident and Prevalent Parkinson Disease

Siegfried Karl Wagner, David Romero-Bascones, Mario Cortina-Borja, et al.

Neurology published online August 21, 2023
DOI 10.1212/WNL.0000000000207727